



Visual Tracking using Kernel Projected Measurement and Log-Polar Transformation

Fateme Bakhshande^a, Hamid D. Taghirad^{b,*}

^a Advanced Robotics and Automated Systems (ARAS), Industrial Control Center of Excellence (ICCE), Faculty of Electrical and Computer Engineering, K. N. Toosi University of Technology, E-mail: f.bakhshande@iee.org.

^b Advanced Robotics and Automated Systems (ARAS), Industrial Control Center of Excellence (ICCE), Faculty of Electrical and Computer Engineering, K. N. Toosi University of Technology, E-mail: taghirad@kntu.ac.ir

ARTICLE INFO

Article history:

Received: December 15, 2014.

Received in revised form:

April 24, 2015.

Accepted: May 29, 2015.

Keywords:

Visual Servoing

Lyapunov Function

Log-Polar Transform

Fourier Transform

ABSTRACT

Visual Servoing is generally contained of control and feature tracking. Study of previous methods shows that no attempt has been made to optimize these two parts together. In kernel based visual servoing method, the main objective is to combine and optimize these two parts together and to make an entire control loop. This main target is accomplished by using Lyapunov theory. A Lyapunov candidate function is formed based on kernel definition such that the Lyapunov stability can be verified. The implementation is done in four degrees of freedom and Fourier transform is used for decomposition of the rotation and scale directions from 2D translation. In the present study, a new method in scale and rotation correction is presented. Log-Polar Transform is used instead of Fourier transform for these two degrees of freedom. Tracking in four degrees of freedom is synthesized to show the visual tracking of an unmarked object. Comparison between Log-Polar transform and Fourier transform shows the advantages of the presented method. KBVS based on Log-Polar transform proposed in this paper, because of its robustness, speed and featureless properties.

1. Introduction

Visual servoing is commonly used for utilizing visual feedbacks to control a robot [1]. Visual servoing (VS) involves moving either a camera or the camera's visual target. The main purpose of VS is to track an object in an unknown environment and to converge the target image to a known desired image. In general, visual servoing consists of two parts: feature tracking and control; in addition, these two parts usually work separately in the close-loop system which uses the vision as the underlying parcel of the loop. VS is usually done without tracking and control optimization. When the robot or object moves, features that are extracted from the image are used as the feedback signal, and control sequence is generated based on these features. Therefore, the problem can be divided into two sub-problems. By this separation, tuning the whole system together is almost impossible. Kernel Based Visual Servoing (KBVS) is presented in this paper to optimize the VS method and to solve the two sub-problems together. The presented method has some superiorities over previous methods such as position-

based and image-based visual servoing [2], [3], 2 1/2 D visual servoing [4] and other advanced methods [5], [6].

In all featureless methods the computational factors decrease because of using all features in the image without shrinking the image into limited extracted features. Extracting features from an image usually requires more computation and also decreases the speed of convergence. KBVS uses the image signal or other transformed image directly to optimize the close-loop system. Spatial kernel-based tracking algorithm [7], [8], [9], [10] is used in this method for designing the feedback controller. The stability of control loop is proven by Lyapunov theory.

Tracking based on kernel is used in [11], [12], [13] for the first time. The most important part in KBVS is designing the kernel function which tunes the performance of control and tracking part. These functions have been defined based on spatial weighted average of the image or transformed image. Therefore, the minimal error of kernel function is used for optimization during the tracking. Swensen and Kallem rendered some kernels for 2D

* Corresponding author, Tel: +982188469084

translation in x-y directions in [12], and also did some experiments on the group of rotations. In [13] Kallem and Dewan proposed a new kernel in depth and roll motions, a Gaussian kernel for depth and a rotationally asymmetric kernel for roll and synthesized them in one kernel. In [11] Swensen and Kallem also analyzed the domain of attraction for some selected kernels through a comparison study. They designated the domain of attraction by acquiring larger area in which the Lyapunov function is positive and its time derivative is negative definite.

In this paper KBVS implementation in four degrees of freedom is presented based on image, Fourier and Log-Polar transform traits. Previous work on 2D translation is first explained, the method for translation along and rotation about the z-axis are then elaborated by using Fourier transform. Besides the innovative method based on Log-Polar transform is presented in two degrees of freedom and full tracking in four degrees of freedom has been implemented. Furthermore, convergence toward the goal position is analyzed by Lyapunov theory. Experimental results verify suitable performance of the proposed method implemented on four degrees of freedom. Numerical results verify the preference of Log-Polar transform that is presented in this paper in comparison with that of Fourier transform in rotation and scale directions.

2. Background Material

2.1. Kernel-based Visual Servoing using Fourier Transform

In this section, KBVS method is explained. First, tracking in 2D translation parallel to the image plane are demonstrated (x,y) which is used for full tracking demonstration. Then, translation along the optical axis (z) and roll about the camera optical axis (θ) have been introduced based on the Fourier transform.

Some assumptions are required in implementation of KBVS. First of all, the camera-robot configurations are assumed as an eye-in-hand configuration. Therefore, it requires fast image processing methods. Besides, a kinematic motion model has been considered for the robot and the joint velocity can be achieved as the control input. Furthermore the camera optical axis is perpendicular to the image plane. Final assumption is that the image scene is continuous and infinite, and also the illumination of the image scene is constant across the image frames. Variation in the illumination of image is considered as the noise signal.

Consider a signal $S(w,t)$ that is the image intensity for each pixel during the time growth. The image at each frame is considered similar to this signal. Kernel projection value is defined as a function of time, called kernel-projected measurement (KPM) or kernel measurement [12]. It can be expressed as follows:

$$\xi(t) = \int_I K(w)S(w,t)dw. \quad (1)$$

In which, $K \in \mathbb{R}^{(n \times 1)}$ is the kernel function. Indeed, the image signal $S(w,t)$ is associated with the 2D translation, scale or rotation in the image which are time variants. $w \in \mathbb{R}^2$ is the spatial index parameter for each image captured by the camera. When the camera moves, the amount of the kernel measurement is changed because $S(.,t)$ varies. Assume that S_0 is the goal value for S and ξ_0 is the goal value for ξ . The objective of KBVS is to drive the robot to the goal position or to force $\xi \Rightarrow \xi_0$. In this section, previous work on 2D translation is first explained, on the basis of which the proposed method for other degrees of motion is then elaborated. Implementation of 2D translation is used for full tracking purpose in order to compare between the proposed method and previous method in other degrees of freedom.

2.2. Translation Parallel to the Image Plane

Assume that the robot moves parallel to a plane, therefore, we have only a 2D translation motion. In this case, the dynamic model for the robot can be expressed as follows:

$$q = u. \quad (2)$$

Where $q=[x,y]^T \in \mathbb{R}^2$ is the position of the end effector and $u \in \mathbb{R}^2$ is the robot control input for each degree of freedom. It is important that the control input is the velocity of end effector. As mentioned above, the purpose of KBVS is to drive ξ toward ξ_0 . Without loss of generality, let us assume that the goal position is ξ_0 which the position of the end effector is $x=0, y=0$. Therefore, the fundamental point is to acquire a control law which drives $[x(t),y(t)]$ toward $[0,0]$. Due to the fact that the distance between the image plane and the target scene is unit, therefore, the motion is in a way that they are parallel and it is correct to say that $S(w,q(t))=S_0(w-q(t))$. Change the coordinate variables by $\bar{w} = w - q(t)$, then (1) can be written as

$$\begin{aligned} \xi(t) &= \int_I K(w)S_0(w - q(t))dw \\ &= \int_I K(w + q(t))S_0(w)dw. \end{aligned} \quad (3)$$

It can be concluded that there is no difference between the case where the kernel is fixed and the image moves or the case where the image is fixed and the kernel moves in the reverse direction. This fact can be used where we need to differentiate ξ . It should be noted that kernel is differentiable but the image signal is not differentiable in some cases.

A Lyapunov function is defined based on KPM error to generate a control law that drives the robot toward the goal position. Hence, a Lyapunov function candidate may be defined as follows:

$$V = \frac{1}{2} \left\| \xi - \xi_0 \right\|^2. \quad (4)$$

Using the chain rule, the time derivative of the Lyapunov function may be derived by:

$$\begin{aligned} \dot{V} &= (\xi - \xi_0)^T \frac{\partial \xi}{\partial t} = (\xi - \xi_0)^T \frac{\partial \xi}{\partial q} \dot{q} \\ &= (\xi - \xi_0)^T \left(\int_I K'(w) S(w) dw \right) u. \end{aligned} \quad (5)$$

Where

$$K'(w) = \frac{\partial K(w)}{\partial w} \in \mathbf{R}^{n \times 2} \quad (6)$$

The following control law ensures that the time derivative of Lyapunov function becomes negative definite.

$$u = - \left(\int_I \nabla K(w) S(w, q(t)) dw \right) (\xi - \xi_0), \quad (7)$$

In which,

$$\nabla K = \frac{\partial K(w)}{\partial w} \in \mathbf{R}^{n \times 2}. \quad (8)$$

And furthermore, the time derivative of Lyapunov function is expressed as:

$$\dot{V} = - \left\| \left(\int_I \nabla K(w) S(w, q(t)) dw \right) (\xi - \xi_0) \right\|^2. \quad (9)$$

2.3. Translation along the optical axis using Fourier Transform

Fourier transform is one of the useful tools in image processing methods which can separate the translation from scale and rotation in image. After applying this transformation on an image, any variations in the translation changes to conversions in the phase of image Fourier transform. Moreover any changes in the scale and rotation are transformed into changes in the magnitude of the image Fourier transform.

In translation along the optical axis the dynamic model for the robot can be expressed as follows:

$$\dot{z} = u. \quad (10)$$

Without loss of generality, let us assume that I_0 is the image signal at $z=0$. Based on this assumption the following equations may be written:

$$I(w, z) = I_0(w/z) \quad (11)$$

$$F(v, z) = z^2 F_0(zv), v \in R^2 \quad (12)$$

KPM is defined by equation (13), and the Lyapunov function candidate can be defined as given in (14). By choosing the control input as (15), time derivative of Lyapunov function becomes negative definite.

$$\xi(t) = \int_I K(v) F(v, z) dv \quad (13)$$

$$V = \frac{1}{2} \left\| \xi - \xi_0 \right\|^2 \quad (14)$$

$$u = \left(\int_I v^T \nabla K(v) F(v, z) dv \right) (\xi - \xi_0). \quad (15)$$

2.4. Rotation about the optical axis using Fourier Transform

As mentioned in section (2.3) Fourier transform will individuate translation in x and y directions from scale and rotation. For rotation about the optical axis the magnitude of Fourier transform is used as the designated signal similar to the scale correction. In this case the dynamic model for the robot can be written as follows:

$$\dot{\theta} = u. \quad (16)$$

Assume that I_0 is the signal image at the goal position ($\theta=0$). Therefore I is a rotated version of I_0 and can be written as:

$$I(w, \theta) = I_0(R_\theta w) \quad (17)$$

In which,

$$R_\theta = \begin{bmatrix} \cos \theta & \sin \theta \\ -\sin \theta & \cos \theta \end{bmatrix} \quad (18)$$

Based on (17) the magnitude of Fourier transform for the rotated image is:

$$F(v, \theta) = F_0(R_\theta v), v \in R^2 \quad (19)$$

The Lyapunov function candidate is defined similar to that of translation along the optical axis. By choosing the control input as (20), time derivative of Lyapunov function becomes negative definite.

$$u = - \left(\int_I v^T \nabla K(v) F(v, \theta) dv \right) (\xi - \xi_0). \quad (20)$$

Where:

$$J = R(\pi/2) = \begin{bmatrix} 0 & 1 \\ -1 & 0 \end{bmatrix} \quad (21)$$

In this paper, the proposed method based on Fourier transform is implemented and the results are shown in the experiment section. Then tracking based on Log-Polar transform is elaborated in the next sections. Numerical results is illustrated in the experimental results for comparison between Fourier transform and Log-Polar transform for VS purpose.

3. Kernel-Based Visual Servoing using Log-Polar Transform

Log-Polar transform (LPT) is a useful tool in image processing because of its properties, particularly its rotation and scale invariance property [16-18]. In this paper Log-Polar transform is used to modify rotation and scale based on one single kernel function. In the following section we introduce Log-Polar transform and its main properties then explain the presented method based on Log-Polar transform.

3.1. Log-Polar Transform

Log-Polar Transform is based on the human visual system. Transformation of retinal image into its cortical projection can be modeled by LPT [14]. It is mostly utilizable in image registration and object recognition. Indeed this mapping is non uniform. Therefore, LPT is a nonlinear sampling method that registers an image from Cartesian space to the polar space. In other words, LPT is a 2D conformal transformation which transform $[x,y] \Rightarrow [\varphi,\alpha]$ around the assigned center $[x_c,y_c]$. Therefore, LPT can transform an image from Cartesian space to the polar space as $I(x,y) \Rightarrow ILP(\varphi,\alpha)$. The mathematical formulation of LPT is as follows [15].

$$\varphi = \log_{base} \sqrt{(x - x_c)^2 + (y - y_c)^2} \quad (22)$$

$$\theta = \tan^{-1} \left(\frac{y - y_c}{x - x_c} \right) \quad (23)$$

in which, (x_c,y_c) is the center pixel of the main image in Cartesian coordinate, (x,y) illustrates sampling pixel in the main image and (φ,θ) denotes the log-radius and the angular position in Log-Polar coordinates. As shown in the formulation of LPT and in the Fig. 1, it is obvious that the radius of this transform treats exponentially by increasing distance from the origin. As a result, angular motion through this transformation remains constant from Cartesian coordinate to the polar coordinate. [15]. Hence, points near the origin are oversampled and by increasing distance from the origin they will be undersampled.

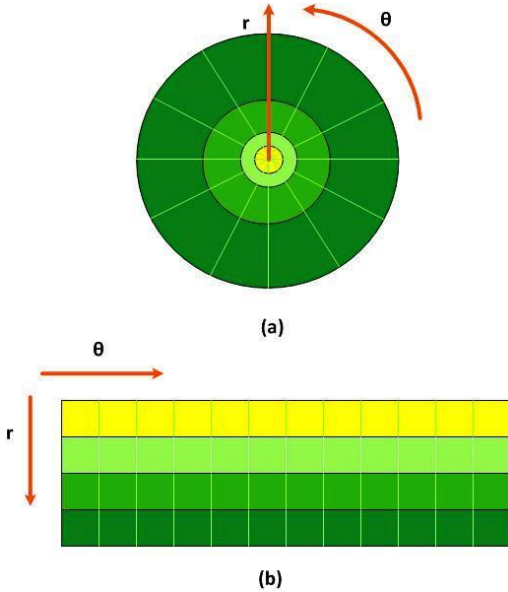


Fig.1: LPT mapping: (a) a paradigm in Cartesian Coordinates, (b) the result by applying Log-Polar Transform in radius and angular direction.

3.2. Extract Rotation and Scale using Log-Polar Transform

In this section we introduce our method which simplify the definition of kernel and convert all degrees of freedom into 2D translation. As shown in Fig. 1, the main property of LPT is that rotation and scale in Cartesian space is turned in shifting along the angular and radial axes in the polar coordinate, respectively. This can be proven based on LPT formulation as follows. Assume that $I(x,y)$ is the main image and $L(x',y')$ is the transformed image of $I(x,y)$ that is rotated α degrees and scaled by size of a [15]. Therefore,

$$\begin{bmatrix} x' \\ y' \end{bmatrix} = \begin{bmatrix} a \cos \alpha & -a \sin \alpha \\ a \sin \alpha & a \cos \alpha \end{bmatrix} \begin{bmatrix} x \\ y \end{bmatrix} \quad (24)$$

$$x' = ax \cos \alpha - ay \sin \alpha, y' = ax \sin \alpha + ay \cos \alpha$$

Consider that $F(\varphi,\theta)$ is the main image in Log-Polar coordinate and $G(\varphi',\theta')$ is the rotated and scaled version of it. Based on (24) we have:

$$\begin{aligned} \varphi' &= \log_{base} \sqrt{(x')^2 + (y')^2} \\ &= \log_{base} \sqrt{a^2 r^2} = \varphi + \log_{base}(a) \end{aligned} \quad (25)$$

And also:

$$\begin{aligned} \theta' &= \tan^{-1} \left(\frac{y'}{x'} \right) \\ &= \theta + \alpha \end{aligned} \quad (26)$$

Therefore based on (25) and (26) it is realizable that rotation and scale in the Cartesian space are transformed into the displacement along the radial and angular axes in the polar space.

In this paper LPT is applied on the main image and the transformed image is used for rotation and scale correction. Furthermore, for detecting movement in radial and angular directions edge detection is applied on transformed image. Furthermore, the edges are used for tracking by using kernel based visual servoing method. Therefore, the previous kernel function in x-y direction can be used for this modification and it does not require any new design for the kernel.

4. Asymptotic Stability

Up to here we have assumed a Lyapunov function candidate that is positive definite and designed a control input that just makes the derivative of Lyapunov function negative semi-definite. Asymptotic stability requires negative definiteness of V' along the traversed trajectory. Without loss of generality we assume that $q_0=0$ is the goal position. Therefore, our aim is to show that V is positive definite and V' is negative definite along the traversed trajectory. To achieve that, use Taylor expansion of $\xi(t)$ about ξ_0 .

$$\xi = \xi_0 + \frac{\partial \xi}{\partial q} q(t) + O(q^2) \quad (27)$$

$$\xi - \xi_0 = Jq(t) + O(q^2) \quad (28)$$

In equation (28) J is Jacobian matrix that may be defined as follows:

$$J = \frac{\partial \xi}{\partial q} = \int \nabla K(w) S(w, q(t)) dw \quad (29)$$

In (27) $O(q^2)$ is higher order derivative terms of q . By assuming a small neighborhood around the goal position, higher order derivatives can be neglected from the Taylor, and therefore, by using equation (28) Lyapunov function and its derivative may be written as follows.

$$V = \frac{1}{2} (\xi - \xi_0)^T P (\xi - \xi_0) \quad (30)$$

$$= \frac{1}{2} q(t)^T J^T P J q(t) + O(q^3)$$

$$Q = J^T P J \quad (31)$$

$$\dot{V} = -q(t) Q Q^T q(t) + O(q^3) \quad (32)$$

In equation (31) P is a $n \times n$ matrix that is positive definite. According to (30) and (32) if Jacobian matrix $J \in \mathbb{R}^{(n \times p)}$ (in which n is the number of kernels and p is the dimension of $q(t)$) is a full column rank, then Q is a full rank matrix with $p \times p$ dimension. By this assumption, it can be concluded that V is positive definite and \dot{V} is negative definite in a small neighborhood around the goal position, and furthermore, they are zero at final destination point. By this assumption asymptotic stability is proven just in a small neighborhood around the goal position. In other cases the higher order in (32) can not be neglected and asymptotical stability is not proven. Experimental results verify asymptotic stability behavior near the goal position. The proposed method is not robust enough against measurement noise therefore in some experiments the uniformly ultimately bounded (UUB) stability could be achieved instead of asymptotic stability.

5. Experimental Results

5.1. System Setup and Implementation Issues

The hardware setup is composed of a PC equipped with a Pentium IV (1.8 GHz) processor and a 512 MB of Ram. Furthermore, the camera is made by Unibrain Company with 30 frames per seconds' rate and a wide lens with 2.1 mm focal length. A 5DOF robot was used to generate the relative cyclic trajectory in the experiments. This robot is a Mitsubishi manipulator model RV-2AJ. Software was implemented in visual studio by using Open CV library which includes image processing algorithms. The robot configuration is shown in Fig.2.

All control inputs are velocities at the end effector level. By using the robot Jacobian matrix at velocity level all control inputs are transformed to joint velocities.

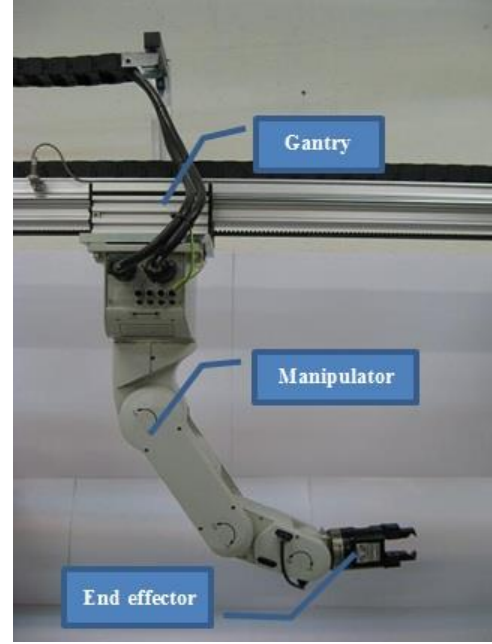


Fig.2: The robot that we used in our experiments, RV2AJ model

For the industrial robots, the control input is not usually executable at the level of joint velocity and the control of the robot is only accessible through the position loop. Furthermore, the robot velocity shall be zero at the start and stop of each motion. Accordingly, the desired velocity that is generated by kernel method can not be directly executed. Consequently, the set of desired velocities are transformed to the desired positions by integration in the appropriate time interval. The time interval shall be carefully selected to have a smooth and continuous motion at the outset. Singularity avoidance and joint velocity limitations are considered for implementation based on motion planner that is formerly presented in [19].

5.2. Implementation of 2D Translation in X and Y Directions

According to the 2.2 the control input is computed based on the kernel function. Kernel functions are usually chosen based on the type of experiments [12], [13]. For 2D Translation kernel functions are designed as follows:

$$K_x(v) = \left(\frac{1}{\sqrt{2\pi\sigma_x}} \right) e^{-\frac{(w_1 - \mu_x)^2}{2\sigma_x^2}} \quad (33)$$

$$K_y(v) = \left(\frac{1}{\sqrt{2\pi}\sigma_y} \right) e^{-\frac{(w_2 - \mu_y)^2}{2\sigma_y^2}} \quad (34)$$

In which, the parameters are set to $\mu_x = \mu_y = -100$, $\sigma_x = \sigma_y = 70$, while (w_1, w_2) is the image index. In Fig.3 three random initials for 2D translation are tested. Suitable convergence toward the goal is shown in this figure, while the mean position errors of x and y are mentioned in Table 1.

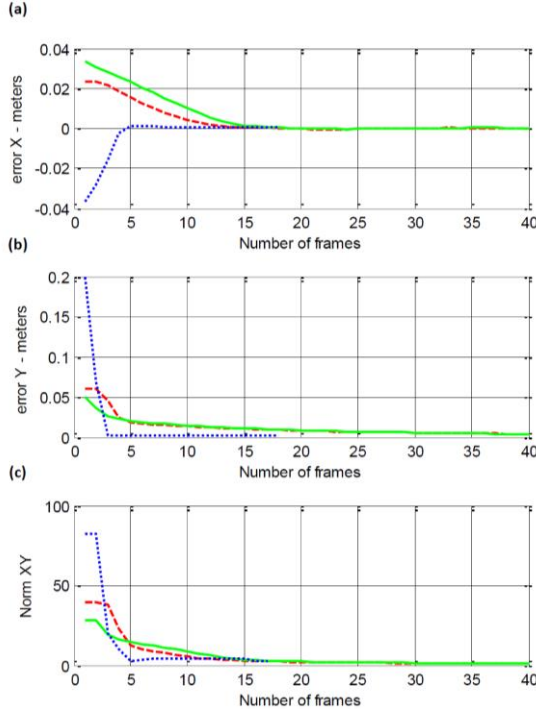


Fig.3: Three experiment results in x-y directions. a) Performance in x axis. b) Performance in y axis, c) convergence of KPM for 2d translation

5.3. Implementation in four degrees of freedom by using FFT

For implementation of KBVS, full tracking in four degrees of freedom is required. Combination of four degrees of freedom requires decomposition of 2D translation from scale and rotation. As mentioned Fourier transform is used for this purpose. Therefore, scale and rotation compensation is done by the magnitude of Fourier transform, and then the image signal is used for tracking in 2D motion.

In this section, some experiments have been conducted to validate the KBVS by using Fourier transform according to the 2-3 and 2-4. We have done some experiments to show the features of Fourier transform in KBVS method. For illustration, some tests in scale and rotation directions and the combination in four degrees of freedom have been designed as follows:

1. Translation along and rotation about the optical axis by computing Fourier transform.

2. Decomposition of 2D Translation from rotation and scale corrections using the magnitude of Fourier transform.

3. Combination of 3D translation (x,y,z) plus roll motion about the optical axis by Fourier transforms.

5.3.1. Depth and Roll Motion Using FFT

Kernel functions for scale and rotation are selected, respectively, as follows:

$$K_z(v) = e^{-\frac{(1/8)\|v\|^2}{2}} \quad (35)$$

$$K_\theta(v) = e^{-\frac{(1/8)v_1^2}{2}} + e^{-\frac{(1/8)v_2^2}{2}} \quad (36)$$

In Fig. 4 five random initials for scale are tested. Suitable convergence toward the goal is shown in this figure, while the mean position errors of scale test are mentioned in Table 2. Fig. 5 shows the five random initials to the goal position for rotation test. Suitable convergence toward the goal is shown in this figure, while the mean position error of θ is mentioned in Table 2. It is obvious in these figures that the performance of kernel based visual servoing system is quite suitable for different initial conditions. In order to verify similar results a compound motion in all degrees of freedom is considered in the next experiments.

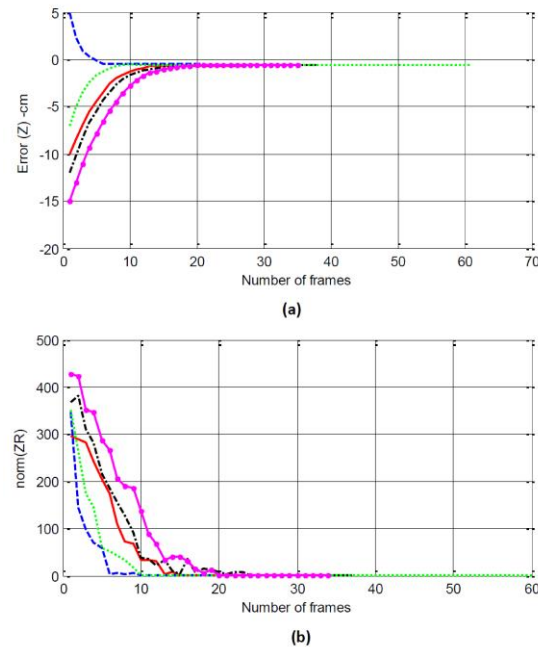


Fig.4: Five experiment results in z directions. a) Performance in z axis. b) Convergence of KPM for z axis using FFT

5.3.2. Decomposition of 2D Translation from rotation and scale corrections

As mentioned before, for 2D translation the image intensity is used directly but for scale and rotation the magnitude of FFT is required. The purpose of this section is to illustrate the effectiveness of FFT in the decomposition of scale and rotation from 2D translation. Note that in both experiments the magnitude of FFT is independent from 2D translation, and therefore, in these experiments the 2D translation error will not be directly compensated.

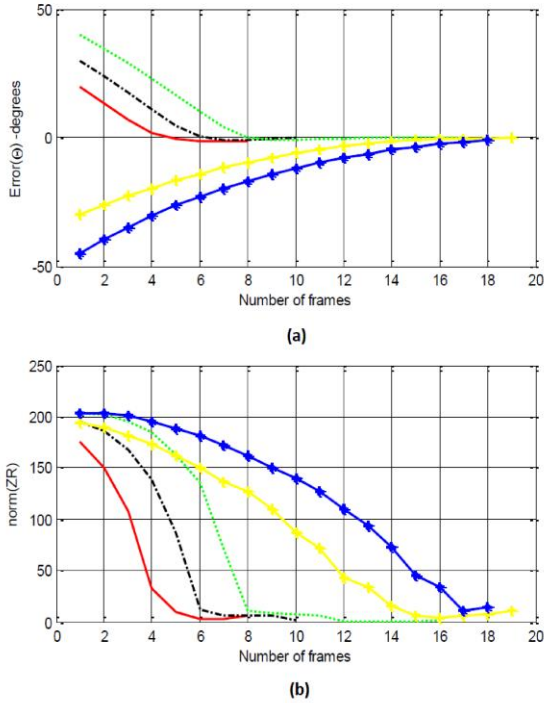


Fig.5: Five experiment results in rotation about z axis a) performance about θ . b) Convergence of KPM for θ using FFT

Fig. 6 illustrates the first experiment where the robot has performed an x-y-z motion. As it is seen in the final picture of this experiment by using FFT of the images in the kernels, the z motion is compensated, but the x and y remains unchanged. Similarly, Fig. 7 illustrates the experiment result for a 3D motion in which in addition to x-y motion rotation along z axis is considered. The same decoupling in motion is clearly observed in the final picture of the target, in which the rotation is compensated for, while the x-y translation is not compensated. Consequently magnitude of FFT is an effective tool to decompose z and θ motions from 2D translation. Therefore, it could be used for KBVS purposes.

5.3.3. 3D Translation + Roll Motion using FFT

For the final experiment we have considered a full 4D motion, in which the 2D translation in x and y motion is performed in addition to a translation along and a rotation about z axis. In order to perform a full visual servoing motion, first the scale and rotation is compensated by using FFT in the kernels, and then the 2D translation is

performed. Fig. 8 illustrates the performance of this experiment, in which the disparity between the final and the goal positions are very small and hard to be observed in this figure. This result verifies the effectiveness of the decomposition method based on FFT image intensity. To verify the result quantitatively, Fig. 9 and Fig. 10 are given. Fig. 9 illustrates KPM for 2D translation, rotation and scale, while Fig. 10 demonstrates the position error norms in all four degrees of freedom. As it is shown in these figures, the tracking errors in all 4 degrees of freedom are relatively small, and remain in suitable range. Relative comparison shows similar and better performance in translational motion compared to that of rotational performance.

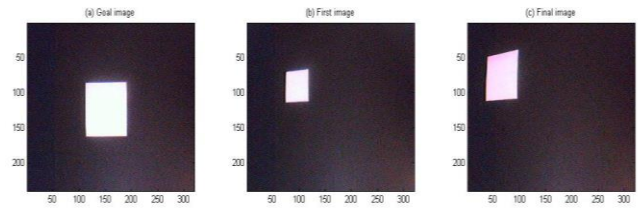


Fig.6: Example images in a real environment. (a). Goal image. (b). initial image with 2D translation and scale. (c). Final image with scale compensation.

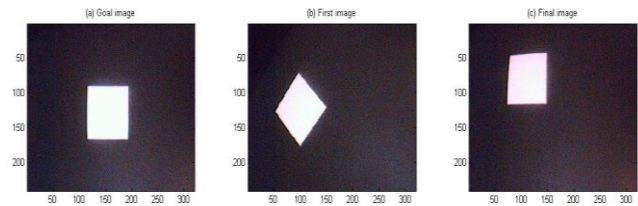


Fig.7: Example images in a real environment. (a). Goal image. (b). initial image with 2D translation and rotation. (c). Final image with rotation compensation.

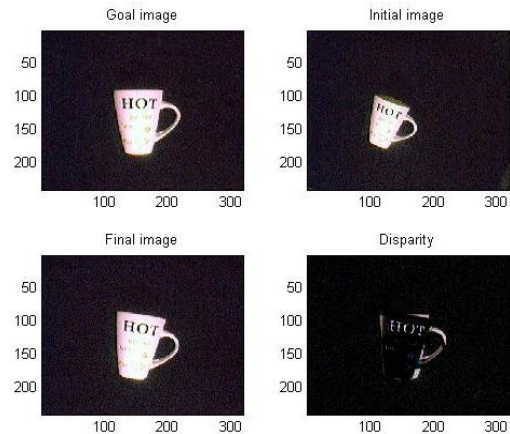


Fig.8: Example images of a 4DOF trial in a real environment. The goal, initial, final and disparity image.

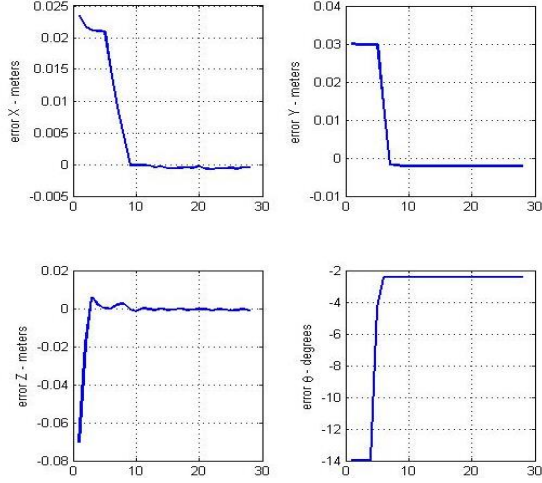


Fig.9: Trial with random initial position, Convergence in X, Y, Z and R motions.

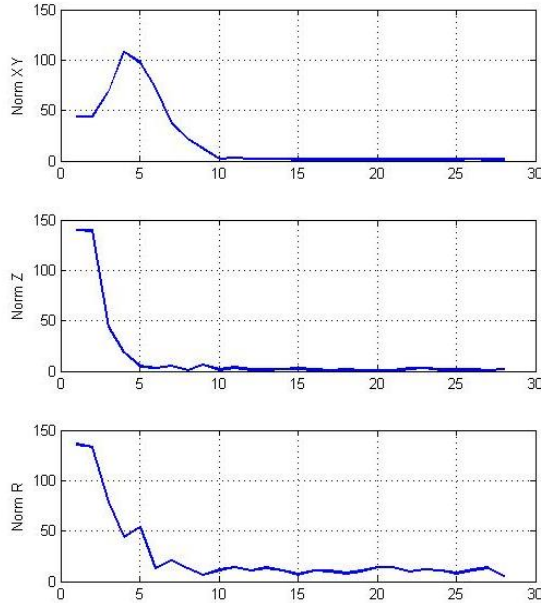


Fig.10: Trial showing control to the goal image shown in Figure(8). a). Convergence in KPM for X-Y. b). Convergence in KPM for Z. c). Convergence in KPM for R.

5.4. Implementation in four degrees of freedom by using LPT

In this section we try to implement the new KBVS method based on Log-Polar transform to illustrate its superiority to the Fourier transform. For this purpose two tests have been designed and implemented on the robot as follows:

1. Depth and roll compensation by computing Log-Polar transform.
2. Combination of 3D translation (x,y,z) plus roll motion about the optical axis by Log-Polar transforms.

The mean position errors of scale and rotation tests are mentioned in Table 2 for more details.

5.4.1. Depth and Roll Motion by using LPT

In this part some experiments have been done on a real object, which is a canister lid in a black background. Some experiments have been performed on random initial position around the goal image.

As mentioned LPT converts an image from Cartesian space to the Polar space. By this transform rotation and scale in Cartesian space convert to the 2D translation in the polar space along the polar axes. Therefore, the 2D translation kernel function can be used in this part. Besides it should be considered that r is the log-radius in the Log-Polar coordinates which treats exponentially by increasing distance from the origin. Therefore, applying 2D translation kernel in this case terminates to unfavorable results. To remedy this problem inverse of the logarithm function is used in KPM, and since the exponential function tends to infinity a tunable parameter a is also considered. Eventually kernel functions are selected as follows:

$$K_z(w_1, w_2) = \left(\frac{1}{\sqrt{2\pi\sigma_z}} \right) e^{-\left(\frac{e^{aw_1} - \mu_z}{2\sigma_z^2} \right)^2} \quad (37)$$

$$(38)$$

In (37) and (38) K_z and K_r are KPM for rotation and scale respectively, $\mu_x = \mu_y = -100$ and $\sigma_x = \sigma_y = 70$. These values have been tuned during the experiments. Other parameters that are tuned for the experiments are controller gains and also a parameter in (37).

Firstly, we consider some initial position in which just the scale translation along the optical axis is performed. Five random initials have been considered and results are shown in Fig. 11. Suitable convergence toward the goal is shown in this figure, while the mean position error of scale test is mentioned in Table 2. Besides we consider rotation about the optical axis and performed for five random initials positions. Results are shown in Fig. 12. Suitable convergence toward the goal has been also observed in this figure, while the mean position error of scale test is mentioned in Table 2. Results in Table 2 show the advantages of using LPT in comparison with FFT. As it is reported in this table, mean position errors significantly decrease using Log-Polar transform.

One of the most important features of using Log-Polar Transform is the combination of scale and rotation correction. As mentioned before, this feature increases the speed of convergence in compared with using Fourier transform. In Fig. 13 three random initials are considered while suitable convergence toward the goal is shown in Fig. 14. It shows correction in roll and depth motion simultaneously for a real object.

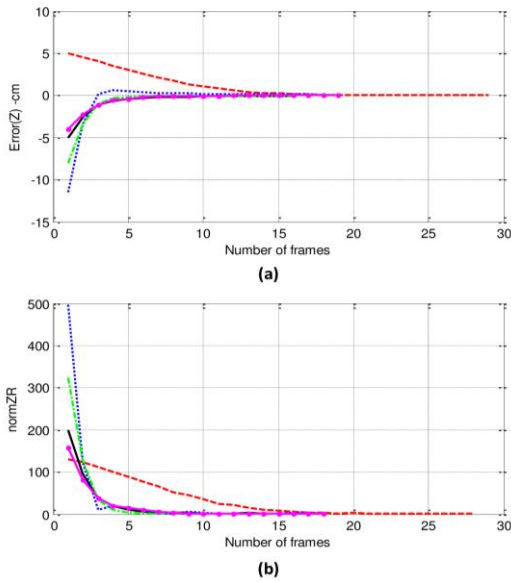


Fig.11: Five experiment results in z directions. a) Performance in z axis. b) Convergence of KPM for z axis using LPT

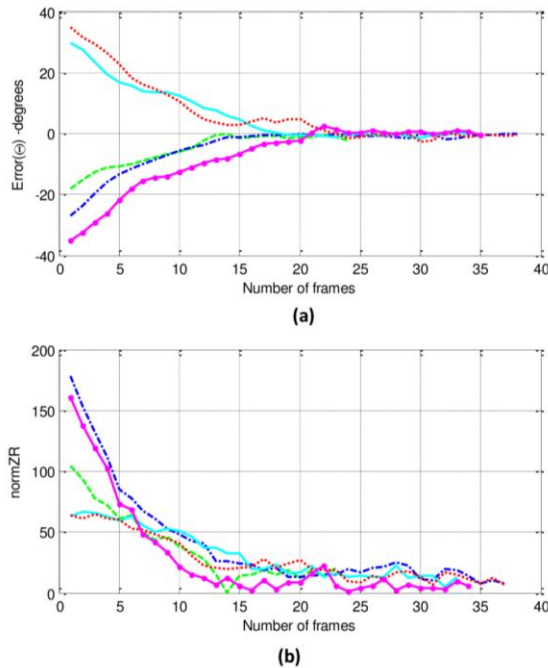


Fig.12: Five experiment results in rotation about z axis a) performance about θ . b) Convergence of KPM for θ using LPT

One of the most important features of using Log-Polar Transform is the combination of scale and rotation correction. As mentioned before, this feature increases the speed of convergence in compared with using Fourier transform. In Fig. 13 three random initials are considered while suitable convergence toward the goal is shown in Fig. 14. It shows correction in roll and depth motion simultaneously for a real object.

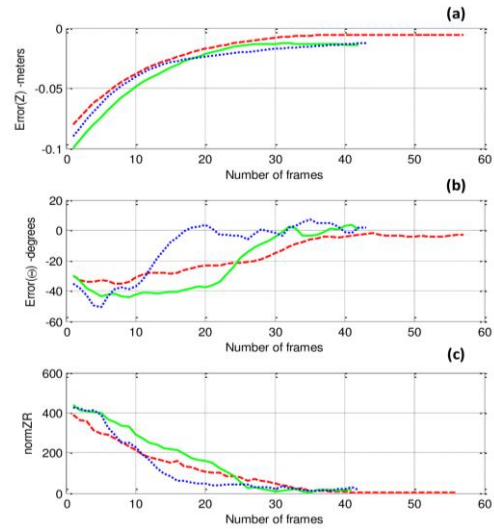


Fig.13: Three experiment results in z and θ directions. a) Performance in z axis. b) Performance in θ axis. c) Convergence of KPM for z- θ using LPT

In this part we try to apply full visual tracking in 3D translation and roll motion by Log-Polar transform. For this purpose the 2D translation has been corrected first. This has been done by finding the contour in the image, approximating its center and shifting it to the center of the goal image. By this means, this image can be used as the new goal image for 2D translation correction. The error threshold can be tuned in addition to the previous tunable parameters to achieve the desired performance. Then the main goal image is considered as the target image and roll and scale correction is performed. Fig. 15 shows the flowchart of sequences performed for visual tracking based on LPT. In Fig. 16 a random initial motion is considered for converging toward the goal image that shown in the Fig. 17.a. It is obvious that based on the error of 2D correction total error could be declined. Furthermore, the error bound could be decreased by improving edge detection algorithm and tuning other parameters.

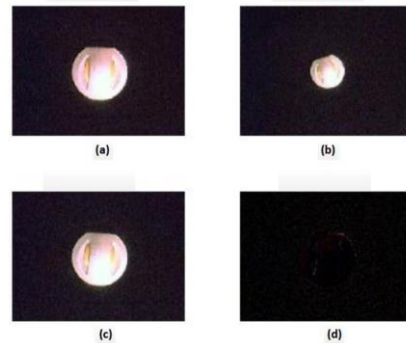


Fig.14: Example images in a real environment. Goal image, initial image, final image and the disparity between initial and final image in rotation and scale correction. LPT

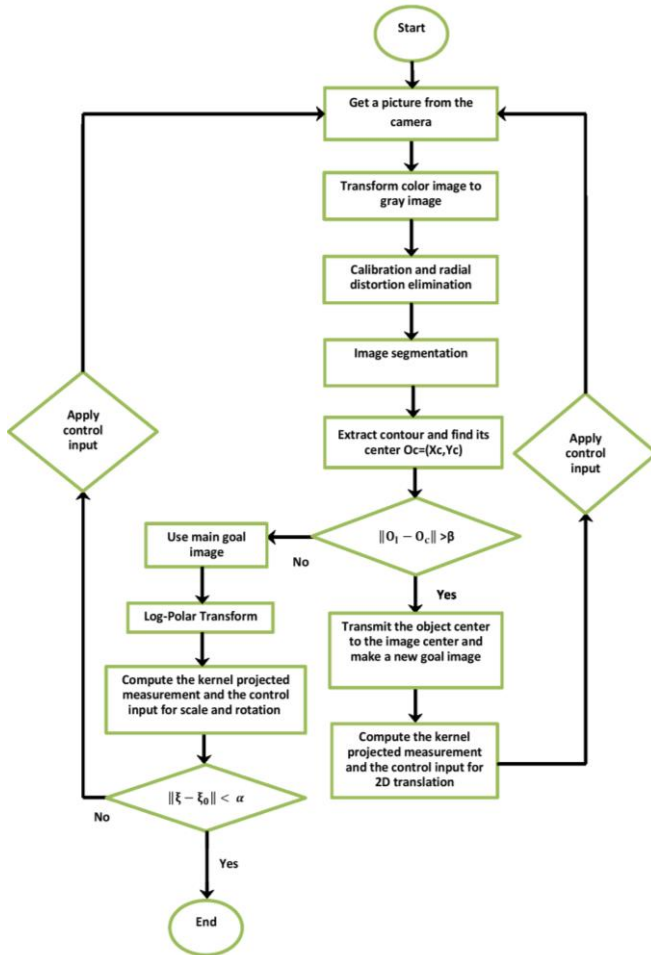


Fig.15: Algorithm of full tracking based on LPT

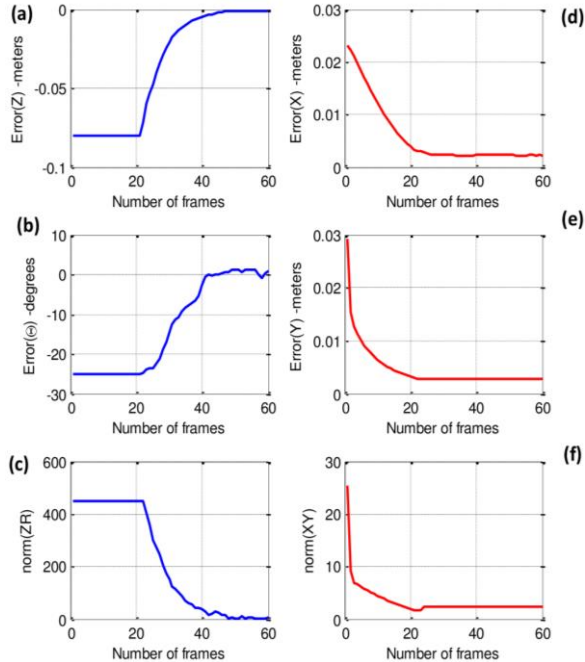
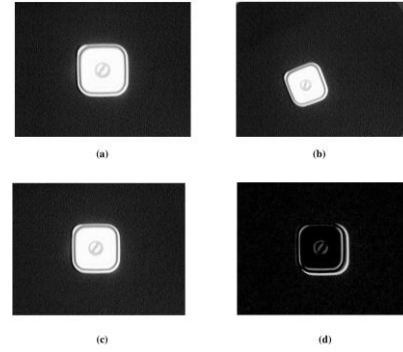

 Fig.16: Trial with random initial position, Convergence in X, Y, Z and θ DOF, Convergence in KPM for z- θ and X-Y


Fig.17: Example images of a 4DOF trial in a real environment. (a). Goal image. (b). Initial image. (c). Final image. (d). Disparity between initial and final image in combination of 3D + roll motion.

Table 1. Results for KBVS method in 2D translation

10 trials with random initial positions	position error
mean position error of x (cm)	0.0205
mean position error of y (cm)	0.1202

Table 2. Comparison of Fourier transform and Log-Polar transform in KBVS

10 trials with random initial positions	position error
mean position error of z (cm)-FFT	0.5158
mean position error of θ (degrees)-FFT	0.2405
mean position error of z (cm)-LPT	0.0263
mean position error of θ (degrees)-LPT	0.0698

6. Conclusions

Kernel based visual servoing is a method in which tracking is performed based on the KPM as the feedback signal which is a weighted sum of the image. KBVS is a featureless tracking method without the need to separate tracking and control parts. Based on the KPM, a Lyapunov function is given to verify asymptotic stability of this method. Consequently the convergence of leading an eye-in-hand robot to the goal position without any feature tracking is verified in experiments. In this paper it is proposed to use Fourier transform to decompose 2d translational motion from the motion along, and rotation about the z-axis. Experimental results verify effectiveness of the proposed method in such decomposition. This idea enables KBVS methods to be concurrently implemented for four degrees of freedom. In the experiments, first the translation along and the rotation about the z axis is compensated by using FFT of image intensity, while at the same time the other 2 degrees of translation are compensated for with the ordinary kernel functions. Besides Log-Polar transform has been introduced to increase the accuracy and speed of convergence. This purpose is done by converting the rotation and scale directions from Cartesian space to the 2D translation in the polar space. Besides compensation in rotation and

scale directions can be done simultaneously with one kernel function. Final experimental results verify suitable tracking performance for tracking an unmarked, and non ideal object in a real environment. Comparison between FFT and LPT shows the superiority of LPT performance in KBVS method.

References

- [1] A. Castano and S. Hutchinson, Visual compliance: Task directed visual servo control, *IEEE Transactions on Robotics and Automation*, 10 (1994) 334-342.
- [2] S. Hutchinson, G.D. Hager, P.I. Corke, A tutorial on visual servo control, 12 (1996) 651-670.
- [3] W.J. Wilson, C.C. Williams Hulls, G.S. Bell, Relative end-effector control using cartesian position based visual servoing, *IEEE Transactions on Robotics and Automation*, 12 (1996) 684-696.
- [4] F. Chaumette and E. Malis, 2 1/2 D visual servoing: a possible solution to improve image-based and position-based visual servoings, *IEEE International Conference on Robotics and Automation*, 1 (2000) 630-635.
- [5] F. Chaumette and S. Hutchinson, Visual servo control, part II: Advanced approaches, *IEEE Robotics and Automation Magazine*, 14 (2007) 109-118.
- [6] D. Kragic and H.I. Christensen, Technical report, *Computational Vision and Active Perception Laboratory*, (2002).
- [7] D. Comaniciu, V. Ramesh, Meerc, *IEEE Transactions on Pattern Analysis and Machine Intelligence*, 25(5) (2003) 564-575.
- [8] M. Dewan and G. Hager, Towards optimal kernel-based tracking, *Computer Vision and Pattern Recognition*, 1 (2006) 618-625.
- [9] Z. Fan, Y. Wu, M. Yang, Multiple collaborative kernel tracking. In *Proc. IEEE Conf. on Computer Vision and Pattern Recognition*, 2005.
- [10] G.D. Hager, M. Dewan, C.V. Stewart, Multiple kernel tracking with ssd, In *Proceedings of the IEEE Conference on Computer Vision and Pattern Recognition*, 1 (2004) 790-797.
- [11] J. Swensen, V. Kallem, N. Cowan, Empirical Characterization of Convergence Properties for Kernel-based Visual Servoing, *Visual Servoing via Advanced Numerical Methods*, Springer-Verlag, (2010) 23-38.
- [12] V. Kallem, J.P. Swensen, M. Dewan, G.D. Hager, N.J. Cowan, Kernel-Based Visual Servoing: Featureless Control using Spatial Sampling Functions.
- [13] V. Kallem, M. Dewan, J.P. Swensen, G.D. Hager, N.J. Cowan, Kernel-based visual servoing, In *IEEE/RSJ International Conference on Intelligent Robots and System*, (2007) 1975-1980.
- [14] H. Araujo and J.M. Dias, "An introduction to the log-polar mapping", *Second Workshop on Cybernetic Vision*, pp. 139 - 144, 2002.
- [15] R. Matungka, "Studies on Log-Polar Transform for Image Registration and Improvements Using Adaptive Sampling and Logarithmic Spiral", 2009.
- [16] K. Palander and S.S. Brandt, "Epipolar geometry and log-polar transform in wide baseline stereo matching", *International Conference on Pattern Recognition*, pp. 1-4, 2008.
- [17] R. Matungka, Y.F. Zheng and R.L.Ewing, "Image registration using adaptive polar transform", *IEEE Transactions on Image Processing*, 18, pp. 2340-2354, 2009.
- [18] R. Montoliu, V.J. Traver and F. Pla, "Log-polar mapping in generalized least-squares motion estimation", *Proceedings of 2002 IASTED International Conference on Visualization, Imaging, and Image Processing (VIIP'2002)*, pp. 656-661, 2002.
- [19] H. Taghirad, M. Shahbazi, F. Atashzar and S. Rayatdoost, "Singular Free Motion Planning in Visual Servoing of Redundant Manipulators", Submitted to *IET Computer Vision*.



Fateme Bakhshande has received her B.S. and M.S. degrees in electrical engineering-control in 2009 and 2011 from K. N. Toosi University of Technology, Tehran, Iran. From 2009 to 2011, she was a member of the Advanced Robotics and Automated Systems team (ARAS) and worked on

the visual servoing.

She is currently working toward her Ph.D. degree at Duisburg-Essen University in Germany.

Now, she is a member of SRS team at Duisburg-Essen University and her research interest is robust and nonlinear control.



Hamid D. Taghirad has received his B.Sc. degree in mechanical engineering from Sharif University of Technology, Tehran, Iran, in 1989, his M.Sc. in mechanical engineering in 1993, and his Ph.D. in electrical engineering in 1997, both from McGill University, Montreal, Canada. He is currently the

chairman of the Faculty of Electrical Engineering, and a Professor with the Department of Systems and Control and the Director of the Advanced Robotics and Automated System (ARAS) at K.N. Toosi University of Technology, Tehran, Iran. He is a senior member of IEEE, and member of the board of Industrial Control Center of Excellence (ICCE), at K.N. Toosi University of Technology, editor in chief of *Mechatronics Magazine*, and Editorial board of *International Journal of Robotics: Theory and Application* and *International Journal of Advanced Robotic Systems*. His research interest is robust and nonlinear control applied to robotic systems.